FATIGUE PROBLEMS OF THE FUTURE: HIGH-CYCLE FATIGUE FAILURES OF SILICON MEMS

C. L. Muhlstein[†], E. A. Stach[††] and R. O. Ritchie[††]

Although fatigue continues to be a major factor limiting the useful life of structural components, one emerging area where fatigue damage is a major consideration is in the design and reliability of microelectro-mechanical systems or MEMS. In this paper, a surprising effect of the fatigue of the micron-scale polycrystalline silicon films used in MEMS is shown. Thin-film silicon is shown to display "metal-like" stress-life fatigue behavior in air, with failures occurring after $>10^{11}$ cycles at stresses as low as half the fracture strength. The mechanisms underlying this effect, which is not seen in bulk Si, are presented, and procedures for limiting the fatigue susceptibility of polysilicon structural films using self-assembled monolayer coatings are discussed.

INTODUCTION

Silicon-based structural films are currently the dominant material for microelectro-mechanical systems (MEMS) because the micromachining technologies are readily adaptable from the microelectronics industry and are compatible with fabrication strategies for actuation and control integrated circuits. Applications range from memory, mass storage, and display applications for personal computing to critical sensor applications such as pressure transducers in medical devices and inertial sensors for passive restraint systems (e.g., airbags) and active automotive suspensions (Fig. 1). As MEMS are emerging from their infancy, it has become clear that micron-scale silicon-based films are currently the dominant structural material for such micromachines, almost to the total exclusion of metallic materials. However, the long-term durability of these structures may be compromised by a susceptibility of thin-film silicon to premature failure by fatigue [1-12].

Cyclic fatigue is the most commonly encountered mode of failure in structural materials [13]. In ductile (metallic) materials, fatigue is attributed to cyclic plasticity involving dislocation motion that causes alternating blunting and resharpening of a pre-existing crack tip as it advances [14]. In brittle (ceramic) materials where dislocation mobility is restricted, fatigue conversely occurs by cycle-dependent degradation of the (extrinsic) toughness of the material in the wake

[†] Department of Materials Science and Engineering, The Pennsylvania State University, University Park, PA 16802, USA
[††] Materials Sciences Division, Lawrence Berkeley National Laboratory, and Department of Materials Science and Engineering, University of California, Berkeley, CA 94720, USA

of the crack tip [13]. As silicon is a brittle material (no dislocation activity is generally observed below ~500°C) with little evidence of extrinsic toughening [15] or susceptibility to environmental cracking [16], it should not fatigue at ambient temperatures. Indeed, there is no evidence that bulk silicon is prone to fatigue failure at all. However, cyclically-stressed micron-scale silicon films are known to fail in room air at stresses well below their (single cycle) fracture strength [1-12].

Although first reported a decade ago [1], the mechanistic origins of such thin-film silicon fatigue have remained elusive. Speculations have included static fatigue of the native oxide [1,8], dislocation activity, impurity effects, and stress-induced phase transformations, although there has never been any conclusive evidence to support these mechanisms, nor any direct observations of fatigue damage and how it accumulates.

In this paper, we show evidence [11,12] that the cracking processes associated with the fatigue of thin-film silicon are confined solely to the native oxide layer, and present a mechanism for such behavior involving sequential oxidation and moisture-assisted cracking in this amorphous layer. Additionally, we suggest a method for suppressing the fatigue of silicon through the use of alkene-based, self-assembled monolayer coatings that inhibit the formation of the native oxide layer.

MATERIALS AND EXPERIMENTAL PROCEDURES

The thin films examined were low-pressure chemical vapor deposited (LPCVD) n^+-type polycrystalline silicon, fabricated as 2-μm thick films using the MCNC/Cronos MUMPs™ process. Wafer curvature measurements indicated a compressive residual stress of ~9 MPa. Secondary ion mass spectroscopy revealed the presence of $\sim 2\times10^{18}$ $^{atoms}/_{cm^3}$ hydrogen, 1×10^{18} $^{atoms}/_{cm^3}$ oxygen, and 6×10^{17} $^{atoms}/_{cm^3}$ carbon [6]; in addition, 1×10^{19} $^{atoms}/_{cm^3}$ of phosphorous were detected from the phosphosilicate glass used for doping. The films, which were representative of those used throughout micromachining and MEMS research and production, had a Young's modulus of 163 GPa and a Poisson's ratio of 0.23. Fracture strengths typically ranged from 3 to 5 GPa, depending on loading condition, specimen size and test technique, with a fracture toughness, K_c, of ~1 MPa$\sqrt{m}$ [15].

Microstructures were characterized with transmission electron microscopy (TEM), using cross-sectional specimens prepared from patterned films, and plan view observations by direct imaging of the full thickness samples. Diffraction contrast and high-resolution microscopy was performed using a 800 kV JEOL Atomic Resolution Microscope, a 300 kV JEOL 3010 TEM, and a 1.0 MeV Kratos High Voltage Electron Microscope (HVTEM). Analytical characterization was conducted with a Philips CM200 Field Emission microscope with a Link Energy Dispersive Spectrometer, a Gatan Image Filter for electron energy loss spectroscopy EELS) and energy filtered imaging (EFTEM).

The film microstructures were found to have an equiaxed grain morphology (grain size of ~100 nm), with no strong texture. EELS and EFTEM imaging suggested no segregation of O, C, P or N, or precipitation of secondary species. Diffraction contrast imaging revealed several types of lattice defects, including microtwins, stacking faults and Lomer-Cottrell dislocation locks (Fig. 2).

To determine the fatigue life as a function of applied stress, a notched cantilever beam specimen within a micron-scale "on-chip" fatigue characterization structure (~300 μm square) was used (Fig. 3) [4-6]. Polysilicon samples were prepared by removing the sacrificial oxide layer in 49% hydrofluoric acid (HF) for 2½ - 3 min, drying at 110ºC in air, and mounting in ceramic electronic packages. The notched beam specimen (~40 μm long, 19.5 μm wide, and 2 μm thick, with a 13 μm deep notch with ~1 μm root radius), was attached to a large, perforated plate that served as a resonant mass. The mass and beam were electrostatically forced to resonate and the resulting motion measured capacitively. This generated fully-reversed, constant-amplitude, sinusoidal stresses at the notch, i.e., a load ratio (ratio of minimum to maximum load) of $R = -1$, that were controlled to better than 1% precision. Specimens were cycled to failure at resonance with a frequency of ~40 kHz in ambient air (~25ºC, 30-50% relative humidity) at stress amplitudes ranging from 2 to 4 GPa, using the control scheme described in refs. [5,6].

The specimen compliance, computed from change in the natural frequency of the system [6,17], was monitored *in situ* to evaluate the evolution of damage in the sample from cracking and oxide formation. Experiments using an unnotched specimen demonstrated that changes in resonant frequency are a result of such damage and are not due to variations in temperature, relative humidity or accumulation of debris [8]. The relationship between stresses in the vicinity of the notch and its dynamic response was determined using finite element modeling. Such methods were also used to evaluate the natural frequency, compliance, crack length, and stress-intensity factor, K, for structures containing cracks. The numerical models were constructed [17] using a commercial software package (ANSYS v 5.7).

RESULTS

Stress-life (*S/N*) data for the polysilicon films are shown in Fig. 4a, based on a total of 28 specimens tested in room air [6]. The silicon films can be seen to display "metal-like" *S/N* behavior, with an endurance strength at 10^9 - 10^{10} cycles of roughly half the (single-cycle) fracture strength. Similar behavior has been seen in 20-μm thick films of single-crystal silicon cycled under identical conditions [5]. The change in resonant frequency of the specimens was monitored during testing to provide a measure of the specimen compliance. The frequency decreased (by up to 50 Hz in the long-life tests) before eventual specimen failure at the notch; indeed, using plane-stress finite element modal analyses with ANSYS [6,17], this was

related to the stable propagation of a crack (Fig. 4b). This analysis implies cracking is occurring on length scales commensurate with the native oxide thickness. Estimates of the crack length (Fig. 4b) revealed crack sizes always less than 50 nm.

SEM and TEM of failed specimens established that overload fracture in the films occurred by transgranular cleavage, with evidence of secondary cracking and microcracking. Although SEM studies were inconclusive in discerning differences between these and the fatigue fractures, this was clearly evident in the HVTEM. Examination of fatigue and untested control samples revealed a stark difference in the native oxide at the notch root. In control samples, a ~30 nm thick layer of oxide was uniformly distributed over the sample surfaces (including the notch); in the fatigue samples, however, the oxide layer at the notch was a factor of three thicker (Fig. 5a). As *in situ*, high-resolution infrared imaging of the fatigue sample revealed no changes in temperature greater than 1 K at the notch root during testing, the enhanced notch-root oxidation appeared to be mechanical in origin [11,12]. The precise nature of this effect is unclear, but appears to be related to such processes as stress-assisted diffusion and cracking within the notch oxide layer which permits the further ingress of moisture and continued oxidation in this region [18].

Despite uncertainty in the origin of this layer, its role in thin-film silicon fatigue is clear. By interrupting fatigue specimens prior to failure and examining them with HVTEM, several small growing cracks (on the order of tens of nanometers in length) were observed within the native oxide at the notch root (Fig. 5b). The size of these cracks was consistent with the compliance change predicted by the finite element modeling.

It is believed that the cracking in the oxide layer is environmentally-induced due to the moisture in the air. Since the fracture toughness of the SiO_2 ($K_c \sim 0.8$ MPa$\sqrt{m}$) is comparable to that of silicon ($K_c \sim 1$ MPa$\sqrt{m}$), the oxide would not crack prematurely. However, unlike silicon, amorphous SiO_2 is susceptible to environmentally-assisted cracking in moisture; indeed, the threshold stress intensity, K_{scc}, for such cracking is much less than K_c, i.e., $K_{scc} \sim 0.25$ MPa$\sqrt{m}$, in contrast to silicon where $K_{scc} \approx K_c$ [16]. Since no phase transformations or dislocation activity were detected, the fatigue of Si films in ambient air is deemed to be associated with the moisture-induced cracking in the native oxide layer that has been thickened under cyclic loading – a process that we term *reaction-layer fatigue* (Fig. 6).

In situ measurements of the change in natural frequency during the fatigue test were used to determine the crack length and hence the crack-driving force at failure; this provides a measure of the fracture toughness, which was computed to be ~0.85 MPa$\sqrt{m}$, consistent with that of the native oxide [17]. However, it is important to note the relationship between the critical crack size at final failure, a_c, where $K = K_c$, and the thickness, h, of the SiO_2 layer. Such critical crack sizes are estimated in Fig. 7 for the range of applied stresses used in this study. It is apparent

that for applied stresses of 2 to 4 GPa, which caused failure in the present films after 10^5 to 10^{11} cycles, the critical crack sizes are less than 50 nm, i.e., comparable the observed oxide layer thicknesses, i.e., $a_c \leq h$. *This indicates that the entire fatigue-crack initiation and propagation process and the onset of catastrophic (overload) failure all occur within the oxide layer.*

DISCUSSION

The cyclic fatigue of brittle materials is caused by the degradation of extrinsic toughening mechanisms in the crack wake [13]. Such toughening arises from crack-tip shielding, which in brittle ceramic materials generally results from mechanisms such as grain bridging. Under cyclic loading, frictional wear in the sliding grain boundaries can lead to a decay in the bridging stresses [13,19,20]. The fatigue of brittle materials is therefore associated with intergranular failure. When such materials fail transgranularly, there is little susceptibility to fatigue. Since polysilicon fails transgranularly with little evidence of extrinsic toughening, it would not be expected to be prone to fatigue. Similarly, below ~500°C, there is no evidence of mobile dislocation activity [21], which could cause fatigue failure as in a ductile material.

In this study, we have shown that the fatigue susceptibility of thin-film silicon is associated with a conceptually different mechanism, that of sequential mechanically-induced oxidation and environmentally-assisted cracking of the surface layer of native oxide that forms upon reaction with the atmosphere. This reaction-layer fatigue mechanism was observed experimentally as a continuous decrease in the specimen stiffness during fatigue loading [6] and was visualized directly using HVTEM. The native oxide, which initially forms on the exposed silicon surface, thickens in high stress regions during cyclic loading and becomes the site for cracks that grow stably in the oxide layer. The process repeats itself until a critical crack size is reached, whereupon the silicon itself fractures catastrophically. The rate-dependence of thin-film silicon fatigue is thus dictated by the cycle-dependent oxide thickening process and the time-dependent moisture-assisted subcritical crack growth in this oxide layer.

This mechanism applies equally to bulk as well as thin-film silicon, even though bulk silicon is not susceptible to either environmentally-assisted cracking or fatigue. This is because cracking in the nano-scale native oxide film would have a negligible effect on a macroscopic sample of silicon under load, since crack sizes in the oxide could never reach critical size, i.e., $a_c >> h$. In contrast, with thin films where the surface-to-volume ratio is far larger such that the oxide layer represents a large proportion of the sample, cracks within the oxide are readily able to exceed critical size and thus can cause failure of the entire silicon component, i.e., $a_c \leq h$.

Of note here is that materials other than silicon may also be prone to reaction-

layer fatigue if they form a surface reaction-layer (upon exposure to service or manufacturing environments) that is susceptible to environmental- or cycle-dependent cracking. *This highlights an important consequence of the reaction-layer fatigue, i.e., that the mechanism can lead to delayed (fatigue) failure of thin films of materials that are ostensibly immune to both environmentally-induced cracking and fatigue in their bulk form*.

An obvious test of this mechanism is to fatigue in an environment where the oxide cannot form. This poses difficulties with the present test system as the removal of the atmosphere affects the damping, causing a mechanical as well as an environmental effect on cracking behavior [17]. An alternative strategy is to use coatings to suppress the formation of the native oxide with the expectation that such samples would not be susceptible to fatigue in air. Accordingly, specific polysilicon specimens in the present study were coated after HF release with a hydrophobic, alkene-based self-assembled monolayer (SAM), 1-octadecene ($C_{16}H_{33}CH{=}CH_2$), which bonds directly to the H-terminated Si atoms on the surface such that no oxide can form (Fig. 8a) [22]. Results on such SAM-coated films definitively show fatigue lifetimes that are far less affected by cyclic stresses (Fig. 8b), thereby providing support for the proposed reaction-layer mechanism of thin-film silicon fatigue.

CONCLUSIONS

Based on a study of the high-cycle fatigue of 2-μm thick structural films of LPCVD n^+-type polycrystalline silicon for MEMS, the following conclusions can be made:

1. Micron-thick polysilicon can prematurely fail by high-cycle fatigue in room air at 40 kHz, at stresses as low as half the fracture strength for lives $>10^9$ cycles. This presents a significant limitation to the long-term stability and durability of silicon-based MEMS devices.
2. HVTEM of the thin films revealed a native oxide layer some 30 nm thick, which under cyclic loading thickened by a factor of three at the notch root. By periodically stopping tests, stably growing cracks, tens of nanometers in length, were detected in this enhanced notch-root oxide; such cracking was reasoned to occur by moisture-induced stress-corrosion cracking.
3. *In situ* monitoring of the natural frequency of the test structure was consistent with such progressive evolution of damage. Fracture mechanics based calibrations revealed cracks sizes <50 nm, comparable with HVTEM images, implying that the fatigue process, i.e., crack initiation, growth and the onset of catastrophic failure, occurs wholly within the oxide layer.
4. The fatigue of thin-film polysilicon is thus ascribed to a “reaction-layer fatigue” mechanism, involving mechanically-induced oxide thickening and moisture-induced cracking of the resulting oxide layer.

5. The mechanism is also applicable to bulk silicon although its effect is negligible. This is because only in the micron-scale thin films can the critical crack size for the onset of catastrophic fracture (when $K = K_c$) be exceeded by cracks solely within the oxide layer.
6. The fatigue susceptibility of polysilicon films can be suppressed by alkene-based self-assembled monolayer coatings, which bond to the H-terminated Si surface and inhibit oxide formation and further ingress of moisture.
7. In general, the reaction-layer fatigue mechanism provides a process by which materials, that are ostensibly immune to environmentally-induced cracking and fatigue in their bulk form, can fail by delayed (fatigue) failure as a thin film.

ACKNOWLEDGMENTS

This work was funded by the Office of Science, Office of Basic Energy Research, Division of Materials Sciences and Engineering of the U.S. Department of Energy under Contract No. DE-AC03-76SF00098, with additional support for equipment from New Energy and Industrial Technology Development Organization (NEDO), Tokyo, Japan, and Exponent, Inc., Natick, MA. Thanks are due to Drs. S.B. Brown, W. Van Arsdell, R. Maboudian, W.R. Ashurst, M. Enachescu, S. Belikov and R.T. Howe for their support, experimental assistance and helpful discussion.

REFERENCES

(1) Connally, J.A. and Brown, S.B., *Science*, Vol. 256, 1992, pp. 1537-39.

(2) Brown, S.B., Van Arsdell, W. and Muhlstein, C.L., in *Proceedings of International Solid State Sensors and Actuators Conference (Transducers '97)*, Edited by S. Senturia, IEEE, pp. 591-93, 1997.

(3) Muhlstein, C. and Brown, S., in *Proceedings of the NSF/AFOSR/ASME Workshop on Tribology Issues and Opportunities in MEMS*, Edited by B. Bhushan, Kluwer Academic, p. 80, 1997.

(4) Muhlstein, C.L., Brown, S.B. and Ritchie, R.O., in *Materials Science of Microelectromechanical System (MEMS) Devices III*, Edited by H. Kahn, M. de Boer, M. Judy, and S.M. Spearing, MRS, pp. EE5.8.1-8.6, 2000.

(5) Muhlstein, C.L., Brown, S.B. and Ritchie, R.O., *JMEMS*, Vol. 10, 2001, pp. 593-600.

(6) Muhlstein, C.L., Brown, S.B. and Ritchie, R.O., *Sensors and Actuators A*, Vol. 94, 2001, pp. 177-88 .

(7) Kahn, H., Ballarini, R., Mullen, R.L. and Heuer, A.H., *Proc. Roy. Soc. A*, Vol. 455, 1999, pp. 3807-23.

(8) Van Arsdell, W.W. and Brown, S.B., *JMEMS*, Vol. 8, 1999, pp. 319-27.

(9) Komai, K., Minoshima, K. and Inoue, S., *Micros. Tech.*, Vol. 5, 1998, pp. 30-37.

(10) Allameh, S.M., Gally, B., Brown, S. and Soboyejo, W.O., *Materials Science of Microelectromechanical System (MEMS) Devices III*, Edited by H. Kahn, M. de Boer, M. Judy, and S.M. Spearing, MRS, pp. EE2.3.1-3.6, 2000.

(11) Muhlstein, C.L., Stach, E.A. and Ritchie, R.O., *Appl. Phys. Lett.*, Vol. 80, 2002, pp. 1532-34.

(12) Muhlstein, C.L., Stach, E.A. and Ritchie, R.O., *Acta Mater.*, Vo. 50, 2002, pp. 3579-95.

(13) Ritchie, R.O., *Int. J. Fract.*, Vol. 100, 1999, pp. 55-83.

(14) Suresh, S., *Fatigue of Materials*, 2nd ed., Cambridge University Press, Cambridge, England, 1998.

(15) Kahn, H., Tayebi, N., Ballarini, R., Mullen, R.L. and Heuer, A.H., *Transducers '99: 10th International Conference on Solid State Sensors and Actuators*, Elsevier, pp. 274-80, 1999.

(16) Lawn, B.R., Marshall, D.B. and Chantikul, P., *J. Mater. Sci.*, Vol. 16, 1981, pp. 1769-75.

(17) Muhlstein, C.L., Howe, R.T. and Ritchie, R.O., *Mech. Mater.*, 2002, in press.

(18) Fargeix, A. and Ghibaudo, G., *J. Appl. Phys.*, Vol. 56, 1984, pp. 589-91.

(19) Dauskardt, R.H., *Acta Metal. Mater.*, Vol. 41, 1993, pp. 2765-81.

(20) Lathabai, S., Rödel, J. and Lawn, B.R., *J. Am. Ceram. Soc.*, Vol. 74, 1991, pp. 1340-48.

(21) Lawn, B.R., Hockey, B.J. and Wiederhorn, S.M., *J. Mater. Sci.*, Vol. 15, 1980, p. 12.

(22) Ashurst, W.R., Yau, C., Carraro, C., Maboudian, R. and Dugger, M.T., *JMEMS*, Vol. 10, 2001, pp. 41-49.

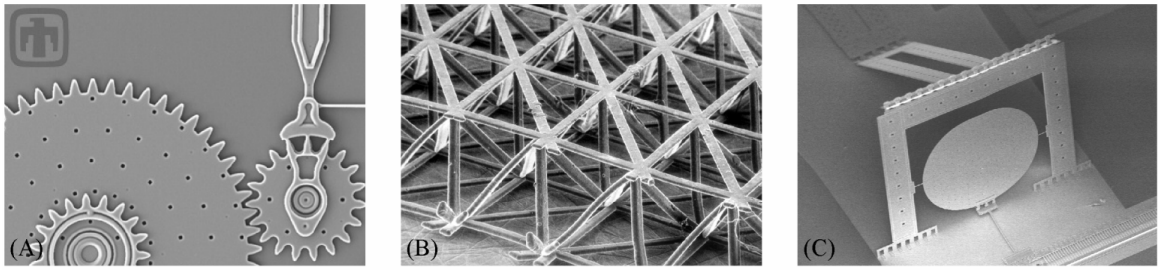

FIGURE 1 Examples of micromachined components. (A) Surface micromachined polycrystalline silicon gears (image Courtesy of Sandia National Laboratories), (B) Nickel microtruss (image courtesy of S. Brittain, Harvard University), (C) Surface micromachined polycrystalline silicon micromirror (image courtesy of R. Conant, U.C. Berkeley).

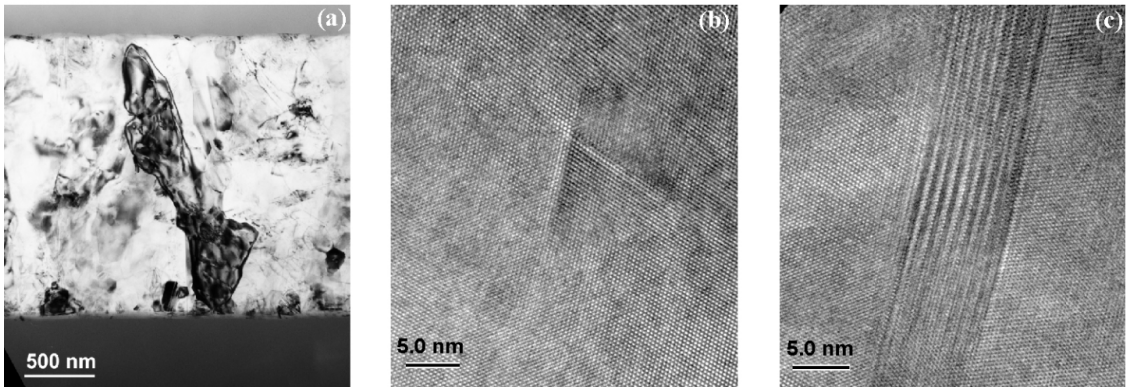

FIGURE 2 Transmission electron microscopy of the microstructure of the polysilicon films, showing (a) cross-sectional TEM image through the film thickness, and HVTEM images of (b) a Lomer-Cottrell lock, and (c) microtwins.

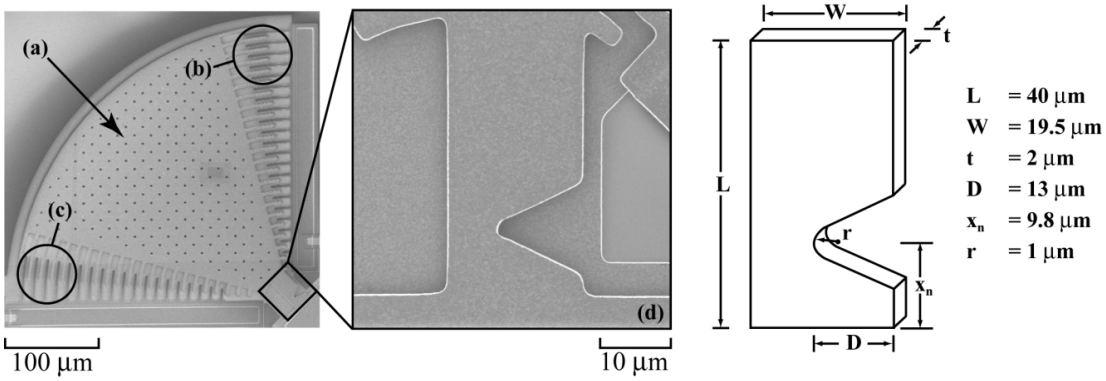

FIGURE 3 SEM of the fatigue test structure and specimen, showing the (a) mass, (b) comb drive actuator, (c) capacitive displacement sensor, (d) notched cantilever beam specimen, and the nominal specimen and notch dimensions.

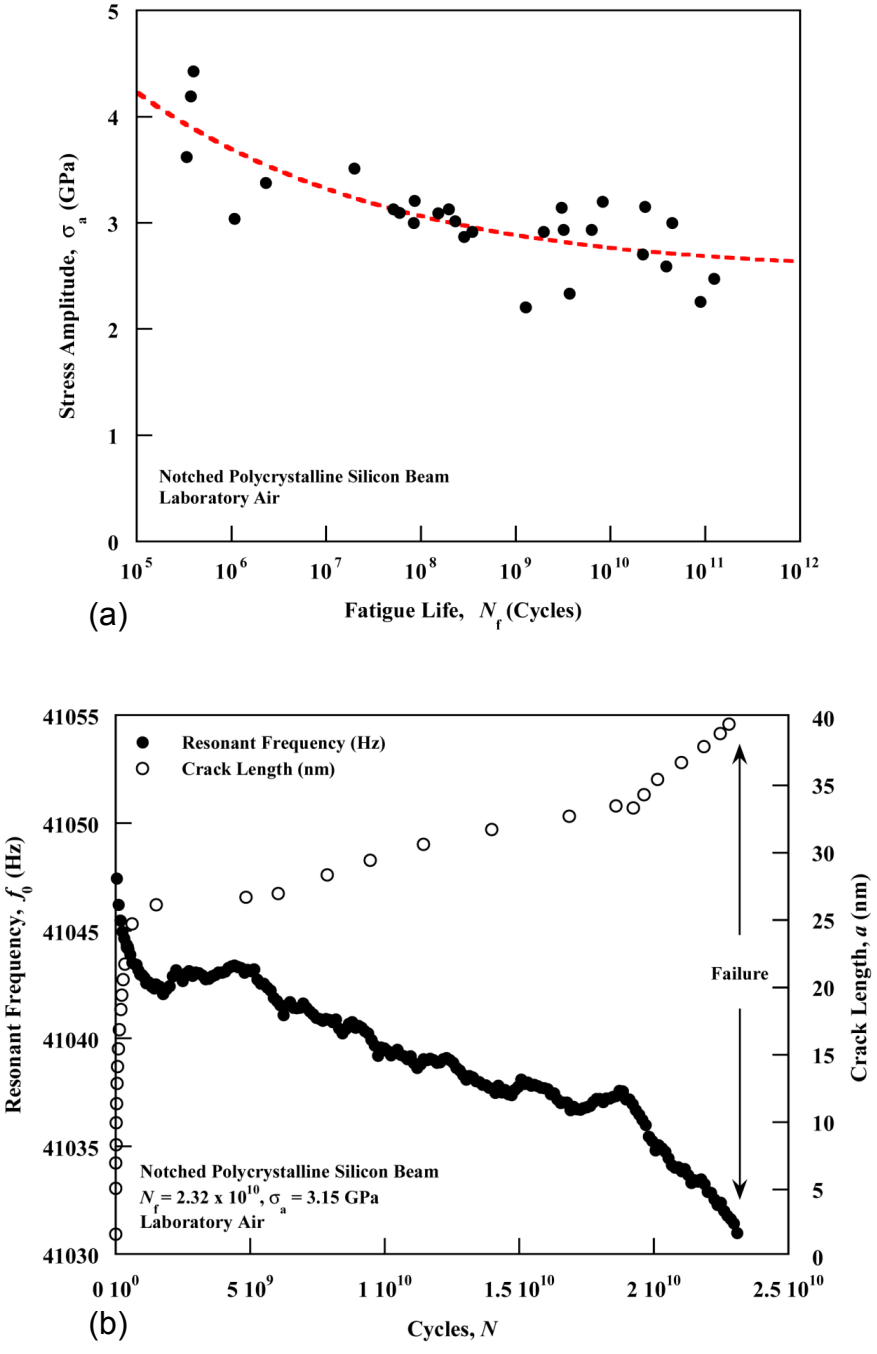

FIGURE 4 (a) Stress-life fatigue behavior of the 2 μm-thick, polysilicon at 40 kHz in moist air under fully reversed loading, and (b) *in situ* damage accumulation in the form of a decrease in resonant frequency, f_{crack}, with time (N_f = 2.23 × 10^{10} cycles at σ_a = 3.15 GPa), with the corresponding calculated increase in crack length, *a*.

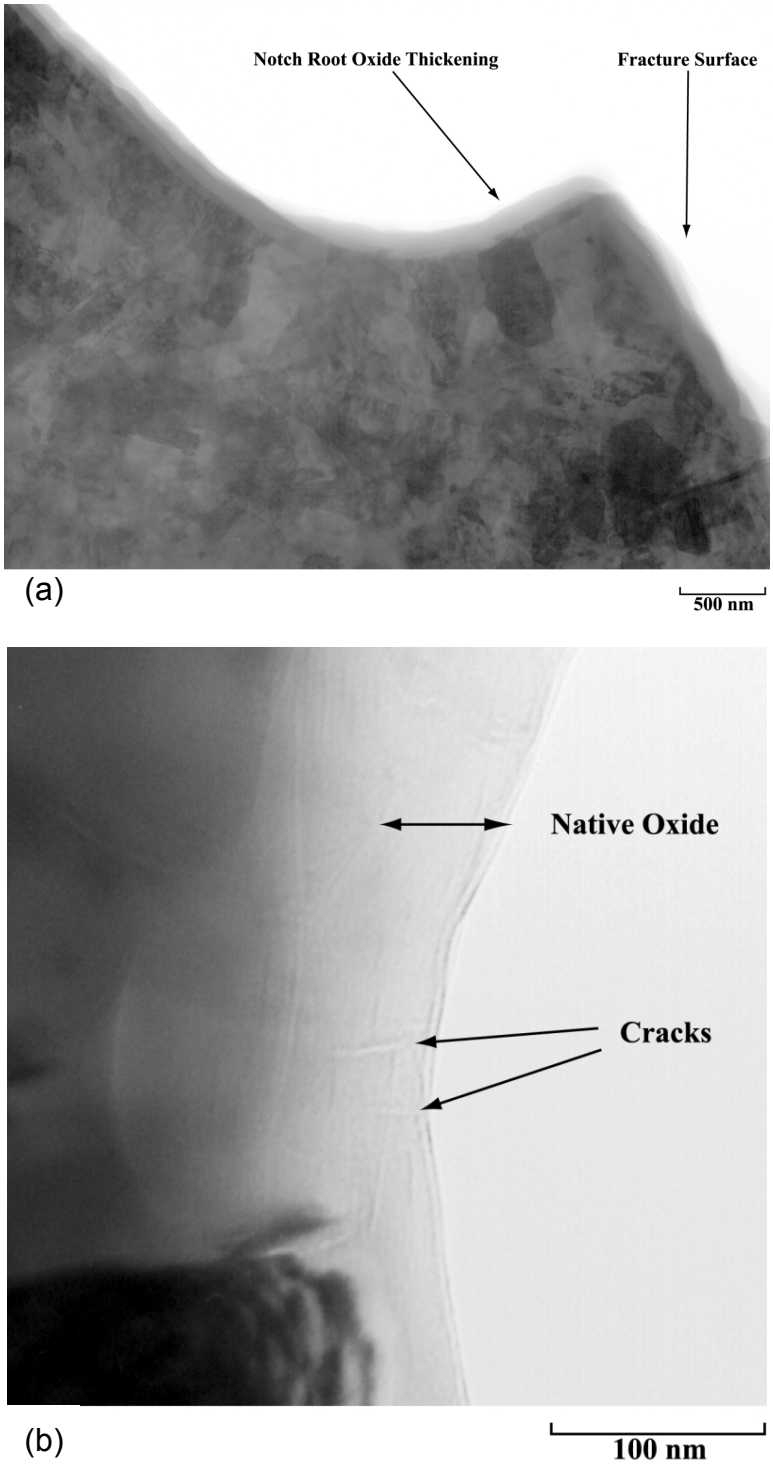

FIGURE 5 HVTEM images of the notch region in an unthinned polysilicon test sample, showing (a) enhanced oxidation at the notch root after cycling, and (b) ~50 nm long stable cracks in the native oxide layer formed during cyclic loading.

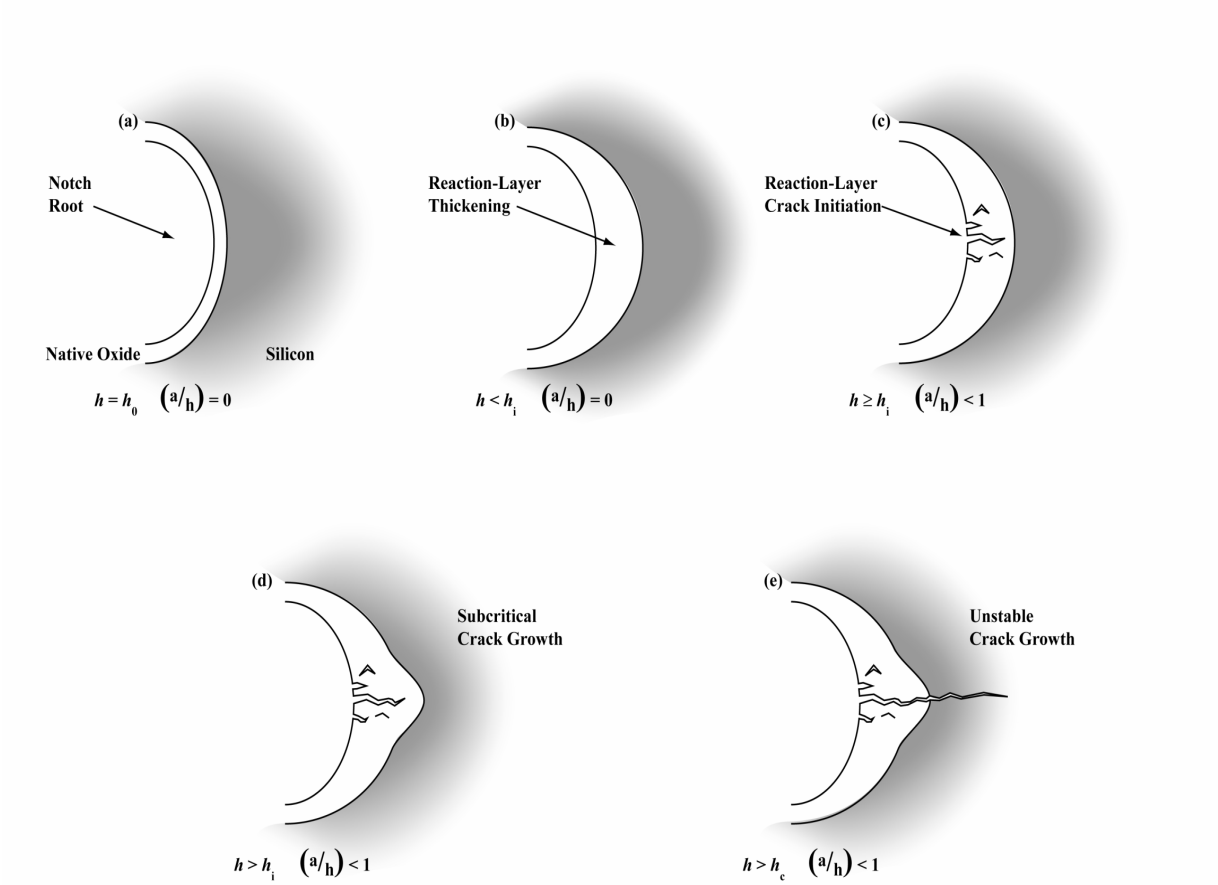

FIGURE 6 Schematic illustrations of the reaction-layer fatigue mechanism at the notch of the polycrystalline silicon cantilever beam. (a) Reaction layer (native oxide) on surface of the silicon. (b) Localized oxide thickening at the notch root. (c) Environmentally-assisted crack initiation in the native oxide at the notch root. (d) Additional thickening and cracking of reaction layer. (e) Unstable crack growth in the silicon film. The thickness of the oxide, h, and relative crack size (a/h) at each stage of the reaction are shown.

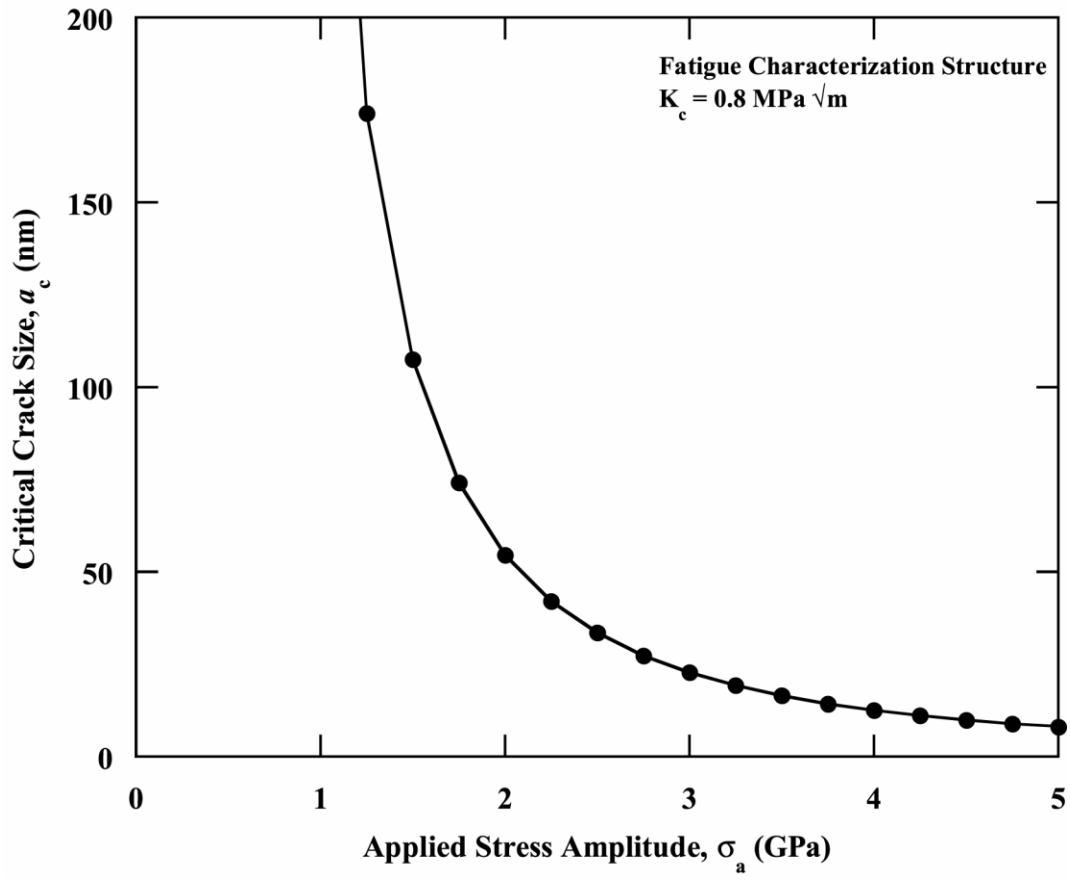

FIGURE 7 Computed estimates of the critical crack size, a_c, as a function of the applied stress amplitude, σ_a, in the fatigue specimens. Critical crack sizes for the stress amplitudes used (σ_a ~ 2 to 4 GPa) are less than ~50 nm, indicating that the onset of final failure of the entire structure occurs within the native oxide.

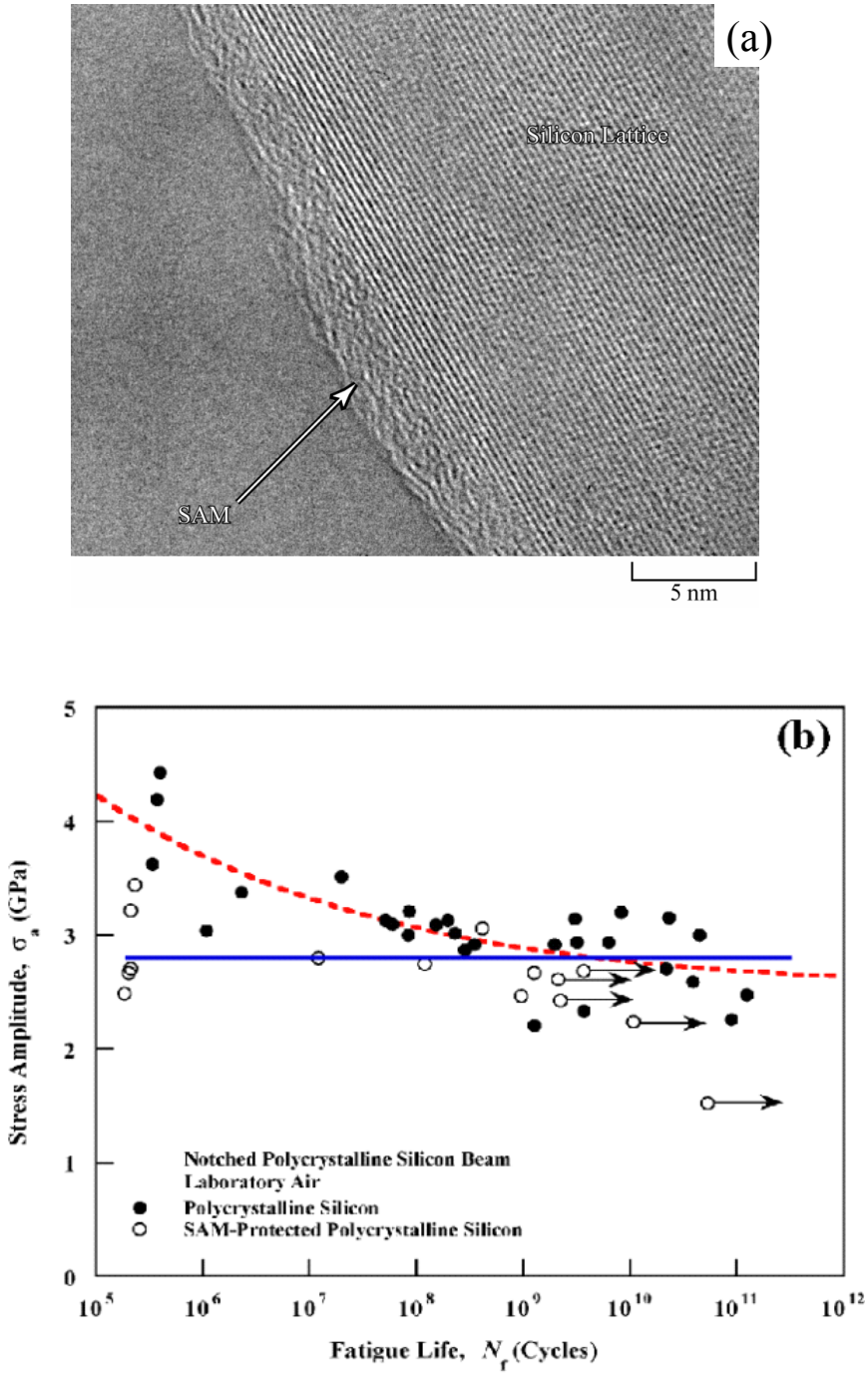

FIGURE 8 (a) HVTEM image showing a 1-octadescene self-assembled monolayer (SAM) coating the root of the polysilicon notch; the absence of the oxide is shown by the lattice fringes of the silicon visible under the ~3 nm layer. (b) *S/N* curves showing the markedly reduced susceptibility of such SAM-coated polysilicon films to fatigue failure.